π^- nuclear capture ratio on hydrogen and oxygen in water

S. Berridge, W. Bugg, Yu. Efremenko, R. Gearhart, and S. Ovchinnikov
University of Tennessee, Knoxville, Tennessee 37996-1200, USA

T. C. Awes and V. Cianciolo
Oak Ridge National Laboratory, High Energy Physics, Oak Ridge, Tennessee 37831-6372, USA

Yu. I. Davydov, T. Numao, and J-M. Poutissou
TRIUMF, 4004 Wesbrook Mall, Vancouver, British Columbia V6T 2A3, Canada
(Received 22 December 2006; published 28 March 2007)

We report on a measurement of the π^- nuclear capture ratio on hydrogen and oxygen in water by two methods. The capture ratio is measured to be $W_{H_2O}=(4.45\pm0.24)\times10^{-3}$.

DOI: 10.1103/PhysRevA.75.034501 PACS number(s): 36.10.−k, 25.80.Hp

The nuclear π^- capture ratio, or fraction of π^- captured on the nucleus of hydrogen or other element X, has been measured in various hydrides H_mX_n [1–3], and studied for its dependence on chemical structure [4–7], and other physical parameters [8,9]. Although these studies have demonstrated that the molecular structure of the compound significantly influences the nuclear π^- capture ratio, the detailed understanding of the mechanism of capture of π^-, which may include capture into Rydberg pion-molecular orbitals, transition to pion-atomic orbitals, and transfer from hydrogen atom to other atom, is far from complete [12–14].

Systematic studies of π^- capture ratios [5,7,9] measured relative to H_2O and CH_2 have enabled measurements with reduced systematic uncertainty. In these studies, the average yield of Refs. [1–3] in CH_2 was assumed to be exactly $W_{CH_2}=12.9\times10^{-3}$ and used for normalization. However, as shown in Table I, there are inconsistencies of up to 70% and 50% in the measured hydrogen capture ratios on CH_2 and H_2O, respectively.

Experimentally, the yield of π^0 from the (π^-,π^0) reaction on hydrides provides a direct measurement of π^- capture on hydrogen because the (π^-,π^0) reaction on the other element in the hydride is forbidden by the negative Q value—e.g., $Q=-8.8$ MeV for ^{12}C and $Q=-5.8$ MeV for ^{16}O.

Two likely sources for inconsistencies in the results are uncertainties in the beam normalization and backgrounds from charge exchange reactions. Earlier experiments, in which the identification of "π^- stop" was done online, could not apply very restrictive criteria and may have been more affected by uncertainties in the beam contamination and the π^- stopping fraction in the sample [2]. Also, many earlier experiments were performed at relatively high energies (60–80 MeV) with beam absorbers that diffused the beam distribution. The use of high-energy pions also increases the probability of charge exchange reactions (π^-,π^0) in flight that cause significant background [10].

In the present measurement of the π^- capture ratio in water, a low-energy pion beam was used to minimize the contribution of charge exchange reactions and the beam composition was carefully monitored. Also, two complementary methods were employed; one was the measurement of π^0 yields from π^- capture by hydrogen (π^0 method), and the other was to fit the high-energy part of the γ-ray spectrum to the expected spectra from radiative π^- capture, $H(\pi^-,\gamma)n$ and $O(\pi^-,\gamma)N^*$ (γ method).

The experiment was performed at the TRIUMF M9A channel. The typical mixture of incoming beam particles at the experimental target was $e:\mu:\pi=88:3:9$ at $P_\pi=70$ MeV/c with a momentum bite $\Delta P/P=\pm4\%$. Figure 1 shows the detector setup. A detailed description of the experimental setup and conditions can be found in Ref. [15]. Incoming pions were identified by two wire chambers (WC1 and WC2) and two plastic scintillators ($B1$ and $B2$), and stopped at a rate of $1-10$ ks^{-1} in an $(8\times60\times60)$-mm^3 purified-water target, tilted by 45°, with a 0.2-mm-thick aluminum frame and two 50-μm-thick Mylar windows. Decay products were observed by two telescope arms at 5 cm from the beam axis at ±90°. Each telescope consisted of three 3–6-mm-thick plastic scintillators ($T1-T3$ or $M1-M3$) and a 46-cm-diam, 51-cm-long NaI(Tl) crystal (TINA) or a 36-cm-diam, 36-cm-long NaI(Tl) (MINA). For γ-ray and π^0 detection, a 5.0-mm-thick 50×50 mm^2 lead sheet was placed as a converter between the first and second plastic scintillators in the MINA telescope, 7 cm from the target center.

The trigger required a beam particle stopping in the target $(B1\cdot B2\cdot\overline{B3})$ with the presence of an outgoing particle into the $M2$ counter that enabled to accept events containing elec-

TABLE I. Various measurements of the nuclear π^- capture ratio on H_2O and CH_2. For the definition of the methods, see the text.

Capture ratio W (10^{-3})		Comments	
H_2O	CH_2	Meth.	Reference
	13.9±1.1	π^0	Chabre *et al.* [1], 1963
2.6±0.4	10.6±1.0	π^0	Dunaitsev *et al.* [2], 1964
	17.9±1.9	π^0	Bartlett *et al.* [3], 1964
3.5±0.6	13.2±1.5	π^0	Krumshtein *et al.* [4], 1968
1.92±1.10	10.6±1.5	γ	Bistirlich *et al.* [10], 1972
	14.5±0.4	π^0	Petrukhin *et al.* [11], 1975
3.9±0.1		π^0	Kachalkin *et al.* [8], 1979
3.52±0.07	12.9	π^0	Harston *et al.* [5], 1991

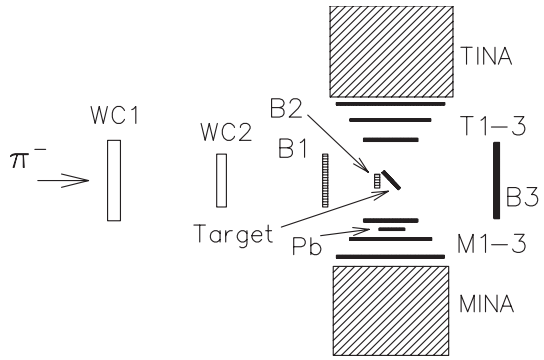

FIG. 1. Experimental setup. TINA and MINA are NaI(Tl) detectors described in the text.

trons, γ rays, and π^0's (two γ rays from $\pi^0 \rightarrow \gamma\gamma$ decay). Beam pions were preferentially selected by their range ($\overline{B3}$ condition), although other beam particles contributed to the online definition of "stop" at reduced rates. Low thresholds on the beam counter signals were used in the online definition of "stop," which allowed better studies of the beam and the background at the expense of an electron contamination of 30–40% in the online "stop" sample. For each data set, a corresponding "beam" trigger ($B1 \cdot B2$) run was taken to correct for electron and muon contamination in the online "stop" definition. Runs with an empty target and with an $8 \times 50 \times 50$ mm^3 beryllium target [$Q=-9.0$ MeV for the (π^-, π^0) reaction] were taken for background measurements. In order to study systematic uncertainties, measurements were also made at beam momenta of 64 ($\sim 1/4$ of pions penetrating into the target), 67, 70 (full penetration into the target), and 73 MeV/c with a 30-mm-diam, 12-mm-thick circular target combined with a 25-mm-diam $B2$ counter without tilting. Runs with positive beam were taken for calibration.

Monte Carlo (MC) calculations [15] were used to simulate the pion beam and π^0 detection. Pions were generated 110 cm upstream of the target, according to the beam profile, and transported to the target. π^-'s were assumed to be captured where they stopped with emission of protons or deuterons according to their respective probability [15].

In the analysis, incoming pions were identified by energy loss in the beam counters $B1$ and $B2$ and time of flight (TOF) with respect to the proton beam bunch. With the above requirements, the electron contamination was estimated to be $<10^{-5}$ of the "π^- stops." Muons originating near the pion-production target were well separated in the TOF spectrum, but those from decay in flight (DIF) upstream of the $B2$ counter were suppressed by the energy loss cuts in the $B1$ and $B2$ counters. The remaining muons including DIF downstream of the $B2$ counter were measured to be 1.6%, which was consistent with the MC estimate of 1.8%. Pions which did not stop in the target but missed the $B3$ counter were estimated to be $\sim 0.2\%$.

In the π^0 method, the π^0 was identified by the presence of a γ-ray signal in MINA ($\overline{M1} \cdot M2 \cdot M3 \cdot$MINA with $E_{MINA} > 11$ MeV) in coincidence with TINA ($E_{TINA} > 21$ MeV). Figure 2 shows typical scatter plots of energies in TINA and MINA for runs taken with H_2O and beryllium targets, respectively. A total of 2311 π^0 events satisfied the π^0 identification window on the energy correlation for the H_2O target. A background of 4% was measured with the beryllium target for the same identification window and subtracted from the H_2O data. The background is mostly due to pion absorption and charge exchange reactions in the beam counters. The π^0 yields were measured over 20 runs with a run-by-run variation of $\sim 3\%$ in the π^0 production rate per "pion stop," consistent with the expected statistical variation. The stability of the beam was also monitored using the accidental peaks for different particle types in the TOF spectrum. The π^0 acceptance was estimated to be $2.16\% \pm 0.13\%$ by MC calculations [15] in which the π^- was "converted" where it stopped to a 2.9-MeV π^0 emitted isotropically. The error in the acceptance derives from the uncertainties in the positions of the counters and the Pb converter. It was estimated by summing in quadrature the efficiency differences, from the standard geometry based on the measured geometry, for displacements of the $M1-M3$ counters, the target, or the lead converter by 2.5 mm, or TINA or MINA by 1 cm toward or along the beam axis, although some changes represent the same effects. The single dominant uncertainty was that of the Pb converter position across the beam axis ($\pm 0.12\%$). The effect of the energy loss cuts in the M counters (around

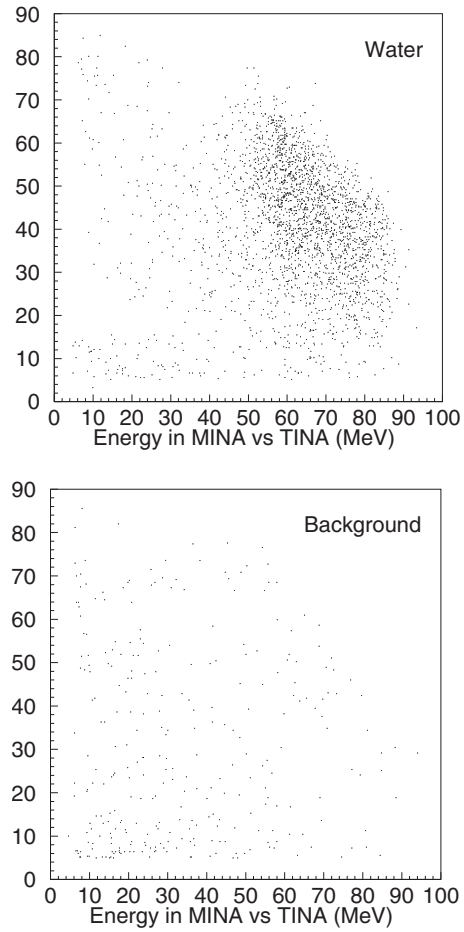

FIG. 2. Energy in TINA vs MINA (MeV) with H_2O and Be (background) targets. The background spectrum corresponds to 1.5 times more pion stops.

20 MeV/cm in energy loss) was estimated to be $<0.02\%$ for data and MC calculations. The dependence on the beam profile was tested by generating beam at the target position using flat and Gaussian distributions with ±2 cm shifts (the beam width parameter of 2 cm of the rms error was consistent with the measured beam distribution). This effect was $<0.03\%$.

MC calculations based on S-wave cross sections [16] for hydrogen and approximate cross sections for carbon and oxygen [17] reproduced the charge exchange background in the $B2$ counter. The nontarget charge exchange reaction background to the π^- capture ratio was measured with the Be target to be 0.05×10^{-3}, while the MC prediction was 0.06×10^{-3}. The additional contribution from charge exchange reactions in the target, which was not in the background subtraction, was estimated to be 0.11×10^{-3} and subtracted from the capture rate—the dominant contribution was from the reaction on hydrogen. Using the Panofsky ratio of 1.546 [18] to compensate for the $\pi^-\mathrm{H}\rightarrow\gamma n$ channel and the total number of 46 664 π^0 events for 1.22×10^9 π^- stops (only 60.9% were valid pions), the capture ratio by the hydrogen atom in water was obtained to be $W^{\pi^0}_{\mathrm{H_2O}}=[4.35\pm0.03(\mathrm{stat})\pm0.25(\mathrm{syst})]\times10^{-3}$.

Capture ratios measured at $P_{\pi^-}=67$, 70, and 73 MeV/c with the circular target were consistent within statistical uncertainties, but the ratio measured at $P_{\pi^-}=64$ MeV/c was $W^{\pi^0}=6.33\times10^{-3}$. In this case, a large fraction of pions (75%) stopped in the $B2$ counter. Correcting this result for the the stopping fraction in the water target gives the capture ratio in $\mathrm{CH_{1.1}}$ (scintillator), $W^{\pi^0}_{\mathrm{CH_{1.1}}}=[6.93\pm0.40(\mathrm{stat})\pm0.58(\mathrm{syst})]\times10^{-3}$.

An alternative measurement method (γ method) was based on the singles γ ray energy spectrum measured by MINA. Since the relative yields of the γ rays from π^- radiative capture reactions by hydrogen and oxygen can be deduced from the γ-ray spectrum fitted with two components, this method is free from possible systematical uncertainties arising from determination of the number of stopped pions in the present experiment and the detection solid angle. Events were selected with the γ-ray signal defined as $\overline{M1}\cdot M2\cdot M3\cdot\mathrm{MINA}$. The crosses in Fig. 3 indicate the energy spectrum of the selected γ rays. The γ-ray spectrum for hydrogen capture was generated by summing γ-ray distributions from the $\pi^-\mathrm{H}\rightarrow\gamma n$ reaction and π^0 decays following the $\pi^-\mathrm{H}\rightarrow\pi^0 n$ reaction weighted with the Panofsky ratio. The γ-ray spectrum for oxygen was generated using the parametrization with nine γ lines and two continuum distributions described in Ref. [19]. The energy resolution of MINA was smeared by 2% to reproduce the positron spectrum from $\mu^+\rightarrow e^+\nu\bar{\nu}$ decays. The result of the fit is shown by the solid histogram in Fig. 3. The dashed (dotted) histogram is the MC simulation of capture on oxygen (hydrogen). The fit for $E_\gamma>50$ MeV corresponds to the oxygen and hydrogen γ-ray ratio of $R_{>50\ \mathrm{MeV}}=4.12\pm0.15$ with χ^2/(degrees of freedom) $=1.66$. The fit using the higher-energy region $E_\gamma>80$ MeV, which excluded the π^0 contribution, was consistent ($R_{>80\ \mathrm{MeV}}=3.90\pm0.25$). The impact of the energy calibration uncertainty of ~1 MeV at 122 MeV was estimated to be ($R_{\pm1\ \mathrm{MeV}}=3.81-4.53$) by shifting the measured spectrum by

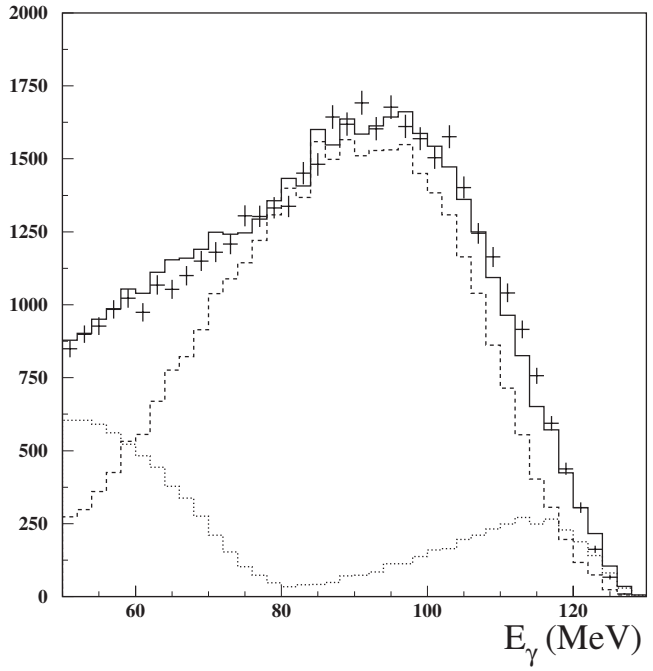

FIG. 3. Energy spectrum of γ rays (counts per 2 MeV) with the H_2O target. The crosses indicate the experimental data. The solid-line histogram is the fit with two components for radiative pion capture on oxygen and on hydrogen.

±1 MeV. Background subtraction using data with an empty target yielded the oxygen-hydrogen ratio 4.08±0.17. Using the radiative capture rate in oxygen to be 2.27±0.24% [19], the nuclear π^- capture ratio in hydrogen after the correction for charge exchange reaction in the target (0.11×10^{-3}) was obtained to be $W^{\gamma}_{\mathrm{H_2O}}=[5.45\pm0.23(\mathrm{stat})\pm0.75(\mathrm{syst})]\times10^{-3}$, where the first error represents the statistical uncertainty in the fit and the second error is due to the uncertainties in the radiative capture rate and the energy calibration.

Apart from the correction for charge exchange reactions in the target, the systematic errors in the two methods are uncorrelated; the uncertainties of the first method are in the acceptance (geometry) and the number of stopped pions, while the second method only depends on the γ-ray energy spectrum and the measurement of radiative pion capture on oxygen. There is a reasonable agreement between the results of the two methods. The combined result is $W_{\mathrm{H_2O}}=(4.45\pm0.24)\times10^{-3}$, which is larger than the previous measurements. Using the ratio between the H_2O and CH_2 measurements [5], the present result corresponds to $W_{\mathrm{CH_2}}=(16.33\pm0.95)\times10^{-3}$ for CH_2, which is 25% larger than the average used for normalization in recent measurements [5,7–9]. The present result for scintillator is also ~15% higher than the linearly interpolated value 6.0×10^{-3} from the averages for $W_{\mathrm{CH_2}}$ and W_{CH} [1–4].

The averages of the previous experiments for $W_{\mathrm{H_2O}}$ and $W_{\mathrm{CH_2}}$ were lowered by a single experiment [2], of which the results were systematically lower by ~20% than the other experiments. A possible source of the difference can be in the method of estimating the stopping fraction of pions in the

target; without energy loss information, the range distribution measurement of beam particles entering the target is likely to be contaminated with muons from DIF, scattered electrons, and protons from nuclear reactions. For the experiments with high-energy pions, the contribution from DIF can be as large as ~12%, as estimated by MC calculations using the geometry of Ref. [1], although the actual DIF fraction varies with the online thresholds of the beam counters and the geometry. In the present experiment, these contributions were well controlled in the offline analysis.

The authors would like to express their gratitude to J. Doornbos for his beam calculations. This work was supported in part by the National Council of Canada, the National Science Foundation, and the Division of Particle Physics and the U.S. Department of Energy under Contract No. DE-AC05-00OR22725.

[1] M. Chabre, P. Depommier, J. Heintze, and V. Soergel, Phys. Lett. **5**, 67 (1963).
[2] A. F. Dunaitsev *et al.*, Nuovo Cimento **34**, 5569 (1964).
[3] D. Bartlett *et al.*, Phys. Rev. **136**, B1452 (1964).
[4] Z. V. Krumshtein, V. I. Petrukhin, L. I. Ponomarev, and Yu. D. Prokoshkin, Sov. Phys. JETP **27**, 906 (1968).
[5] M. R. Harston *et al.*, Phys. Rev. A **44**, 103 (1991).
[6] D. Horváth *et al.*, Phys. Rev. A **44**, 1725 (1991).
[7] A. Shinohara *et al.*, Phys. Rev. A **53**, 130 (1996).
[8] A. K. Kachalkin *et al.*, Sov. Phys. JETP **50**, 12 (1979).
[9] D. Horváth *et al.*, Phys. Rev. A **41**, 5834 (1990).
[10] J. A. Bistirlich *et al.*, Phys. Rev. C **5**, 1867 (1972).
[11] V. I. Petrukhin, V. E. Risin, I. F. Samenkova, and V. M. Surovorov, Sov. Phys. JETP **42**, 955 (1975).
[12] L. I. Ponomarev, Annu. Rev. Nucl. Sci. **23**, 395 (1973).
[13] D. Horváth, Hyperfine Interact. **82**, 483 (1993).
[14] A. Shinohara, J. Nucl. Radiochem. Sci. **1**, 33 (2000).
[15] T. Numao *et al.*, Phys. Rev. D **73**, 092004 (2006).
[16] Numerical values were taken from the Ph.D. thesis of J. Spuller, University of British Columbia, 1978. The original formula can be found in G. Rasche and W. S. Woolcock, Helv. Phys. Acta **49**, 455 (1976). The low-energy cross sections were consistent with the recent publication, W. R. Gibbs and R. Arceo, Phys. Rev. C **72**, 065205 (2005).
[17] G. W. Butler *et al.*, Phys. Rev. C **26**, 1737 (1982). Based on the measurements at T_π=30 MeV for $(\pi^\pm, \pi n)$ reactions, the charge exchange reaction cross section above the threshold energy was assumed to be $3.2(1+B/T_{\pi^-})$ mb for carbon, where B is the Coulomb barrier. The cross section for oxygen was scaled by its mass ratio to carbon to the two-thirds power.
[18] W. K. H. Panofsky *et al.*, Phys. Rev. **81**, 565 (1951); J. Spuller *et al.*, Phys. Lett. **67B**, 479 (1977).
[19] G. Strassner *et al.*, Phys. Rev. C **20**, 248 (1979).